Covalently Interconnected Three-Dimensional Graphene Oxide Solids

— **Source link** ⎘

Parambath M. Sudeep, Parambath M. Sudeep, Tharangattu N. Narayanan, Aswathi Ganesan ...+10 more authors

Institutions: Rice University, Cochin University of Science and Technology,
Indian Institute of Science Education and Research, Thiruvananthapuram, University of Bridgeport ...+1 more institutions

Topics: Graphene oxide paper, Graphene and Nanoporous

Related papers:

- Self-Assembled Graphene Hydrogel via a One-Step Hydrothermal Process

- Three-dimensional flexible and conductive interconnected graphene networks grown by chemical vapour deposition

- Multifunctional, ultra-flyweight, synergistically assembled carbon aerogels.

- Electric Field Effect in Atomically Thin Carbon Films

- Three-Dimensional Self-Assembly of Graphene Oxide and DNA into Multifunctional Hydrogels

Covalently Interconnected Three-Dimensional Graphene Oxide Solids

Parambath M. Sudeep,[†,‡,#] Tharangattu N. Narayanan,[†,#,▲,*] Aswathi Ganesan,[§] Manikoth M. Shaijumon,[§] Hyunseung Yang,[†] Sehmus Ozden,[†] Prabir K. Patra,[⊥] Matteo Pasquali,[∥] Robert Vajtai,[†] Sabyasachi Ganguli,[¶] Ajit K. Roy,[¶] Maliemadom R. Anantharaman,[‡] and Pulickel M. Ajayan[†,*]

[†]Department of Mechanical Engineering & Material Science, Rice University, Houston, Texas 77005, United States, [‡]Department of Physics, Cochin University of Science and Technology, Kochi-682022, India, [§]School of Physics, Indian Institute of Science Education and Research, Thiruvananthapuram-695016, India, [⊥]Department of Biomedical Engineering, University of Bridgeport, Bridgeport, Connecticut 06604, United States, [∥]Department of Chemical and Biomolecular Engineering, Rice University, Houston, Texas 77005, United States, and [¶]Air Force Research Laboratory, 2941 Hobson Way, Wright-Patterson Air Force Base, Dayton, Ohio 45433-7750, United States. [#]These authors contributed equally to this work. [▲]Present address: CSIR-Central Electrochemical Research Institute, Karaikudi-630 006, India.

ABSTRACT The creation of three-dimensionally engineered nanoporous architectures *via* covalently interconnected nanoscale building blocks remains one of the fundamental challenges in nanotechnology. Here we report the synthesis of ordered, stacked macroscopic three-dimensional (3D) solid scaffolds of graphene oxide (GO) fabricated *via* chemical cross-linking of two-dimensional GO building blocks. The resulting 3D GO network solids form highly porous interconnected structures, and the controlled reduction of these structures leads to formation of 3D conductive graphene scaffolds. These 3D architectures show promise for potential applications such as gas storage; CO_2 gas adsorption measurements carried out under ambient conditions show high sorption capacity, demonstrating the possibility of creating new functional carbon solids starting with two-dimensional carbon layers.
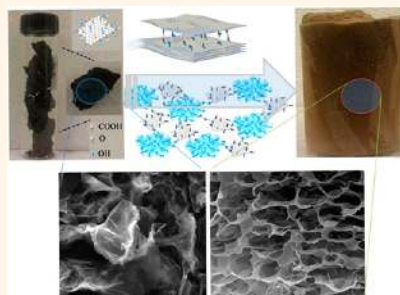
KEYWORDS: graphene oxide · 3D solids · CO_2 adsorption · chemical cross-linking · reduced graphene oxide

Development of 3D hierarchical superstructures (architectures) from interconnected nanoscale building blocks is intriguing for the successful practical use of nanomaterials. Keeping the properties of the individual nanoblocks while constructing macroscopic structures from them still remains a challenge.[1] For example, the macroscopic structures lose scalable properties due to irreversible aggregation or restacking of individual "nanoblocks" during bottom-up processes. Though incorporation of spacers or surfactants can prevent aggregation,[2,3] use of them is limited for the development of ultralow density 3D structures. The covalent linkage between individual building blocks is yet another major challenge in their fabrication. Though challenging, the covalent linkage can bring superior properties to such structures and allow the engineering of these structures to functional solids.[4−6] Recently, some attempts have been made to develop 3D graphitic solid structures such as carbon nanotube solids.[7−12] The junction chemistry in these structures is fundamentally interesting, and

covalent junctions are highly desirable for making stable superstructures.[12]

Graphene oxide (GO) can be extracted through the exfoliation of graphite and contains chemical functional groups on graphene basal planes.[13−18] Promising applications of this in-plane hybrid material containing $sp^2−sp^3$ carbons have been demonstrated.[16−19] Three-dimensional scaffolds from GO have been attempted recently, some of them being hydrogels,[20,21] while others are self-assembled films/aerogels.[22−24] Most of these GO-based solids are obtained through physical interactions of GO building blocks, relying on weak forces such as van der Waals interactions. Several of these process are based on the self-assembly of highly stable GO suspensions during lyophilization with further addition of polymers or other organics to make it mechanically more stable. Very few works have reported[25,26] the chemical cross-linking of GO followed by its reduction to form graphene. However, the resulting structures failed to keep a well-defined 3D morphology, and large-scale synthesis of these materials was challenging.
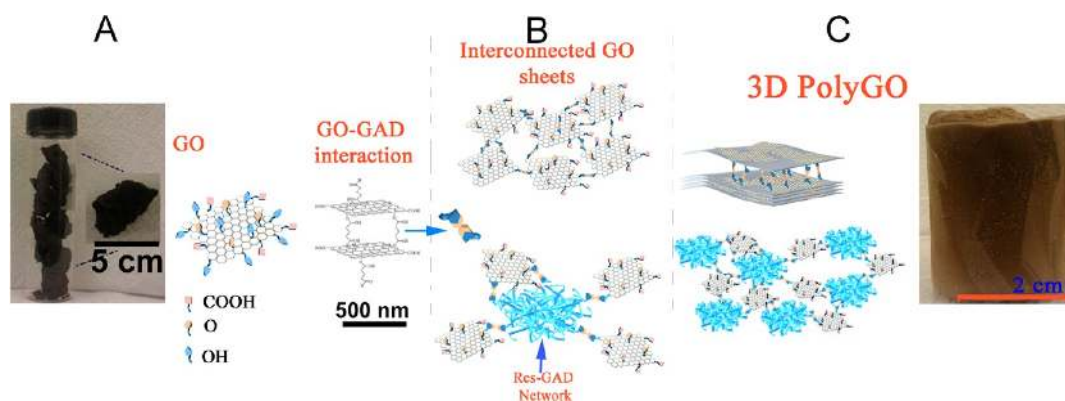
Figure 1. Schematic of the poly-GO synthesis process from initial GO powder. (A) Photograph showing the synthesized GO powders *via* improved technique (left); schematic of GO structure with main functional groups is shown (middle); a possible interaction of GAD with two neighboring GO sheets *via* the −OH groups in GO is also depicted. (B) Schematic of the linkage of GAD (yellow) with two different −OH groups (blue); schematic of two different mechanisms for large-scale GO cross-linking in water solution *via* pure GAD (top) and *via* GAD-Res (bottom). (C) Schematic of the 3D networked structure of poly-GO formed *via* two different mechanisms. Lyophilization (freeze-drying) of cross-linked solution leads to macroscopic solid structures with controllable shape and size.

Recently, reports also demonstrate hydrogels prepared from macroscopic GO self-assembly with DNA.[27]

Here, we report a unique approach to make cross-linked 3D networked GO solids, hereafter called poly-GO. The name has been chosen from the uncanny resemblance of GO sheets with conventional polymer monomer and the cross-linked GO structures considered to be the result of polymerization of individual GO sheets. The interaction of hydroxyl groups in GO with glutaraldehyde (GAD) and polycondensation of GAD and resorcinol (Res) has already been used to make these aerosol-type stable structures. Further, the same method has been adopted to make a cross-linked structure of another material called fluorinated GO (F-GO) (poly-FGO). Controlled reduction of poly-GO will result in the conductive, reduced forms of poly-GO (poly-RGO) while keeping the macroscopic 3D morphology and nanostructure. In addition, to demonstrate the superior properties of these 3D structures for gas storage applications, high pressure CO_2 adsorption studies have been performed on poly-GO samples.

RESULTS AND DISCUSSION

Structural Evolution of Poly-GO from GO. The structural evolution of 3D poly-GO from two-dimensional GO (Figure 2A,B) sheets is shown in Figure 1. Details of the process are given in the Methods section. GO contains various functional groups,[2] particularly the edges are rich with hydroxyl groups (−OH). Glutaraldehyde (GAD) contains two aldehyde groups that can interact with −OH to form hemiacetal structures (Figure 1A, right). Hence, a small amount of GAD at room temperature with magnetic stirring for a few hours can functionalize GO with GAD and can bind two adjacent GO sheets, as shown in Figure 1A. A large number of interconnected structures in water can be formed *via* this with aging (gelation), and removing water from this gelated sample will result in a highly porous
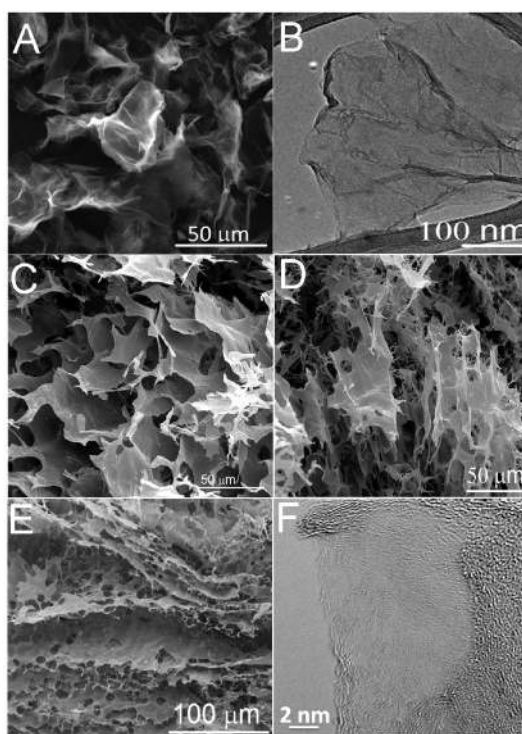
Figure 2. Scanning electron microscopy (SEM) image of (A) GO. (B) Transmission electron microscopy (TEM) image of GO. (C,D) SEM images of poly-GO. (E) SEM image of poly-FGO. (F) High-resolution TEM (HR-TEM) of poly-GO synthesized *via* lyophilization.

interconnected structure (Figure 2C) (further details on the synthesis and microscopic structures are provided in Supporting Information Figure S1 and S2). Variously shaped macrostructures of poly-GO can be molded using various simple cavities (Figure S2 Supporting Information). A proposed mechanism for the formation of Res-GAD gel is shown in Figure S3 (Supporting Information).

The mechanical stability of this structure is further enhanced with the addition of resorcinol (Res) during
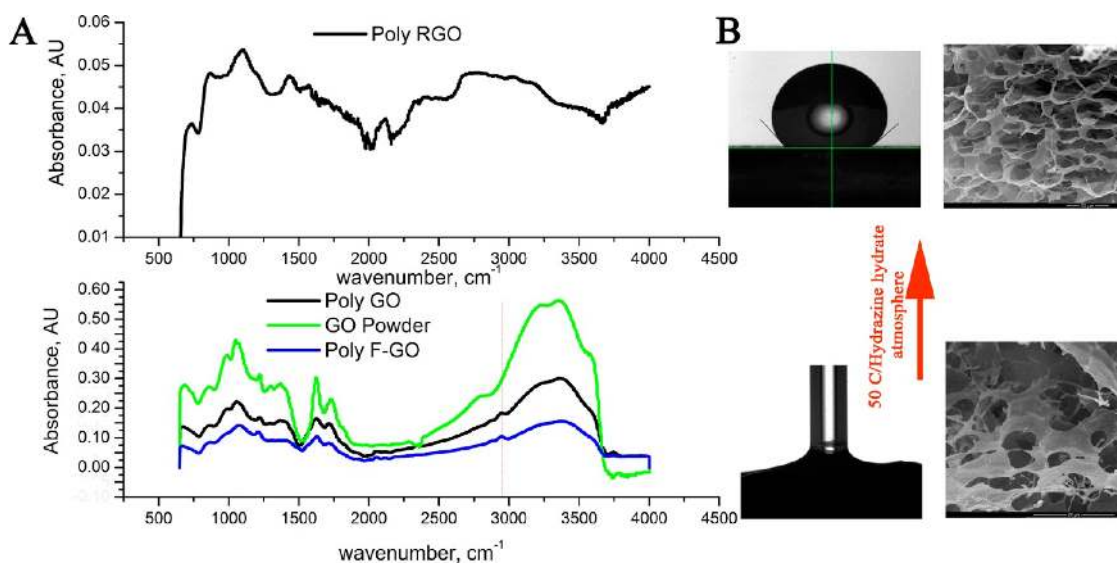
Figure 3. (A) FTIR spectra of various GO samples, (B) contact angle studies on a flat surface of poly-GO shows superhydrophilic nature; the porous section on the surface is shown in the right, whereas its reduced form (poly-RGO) is hydrophobic with a contact angle of ∼110° (top).

GAD addition and initiating Res-GAD sol formation and later the amorphous gelation. A previous report suggests that an ultralow amount of gelating materials can form the gelation only at the edges of GO planes.[25] This can be true due to the large amount of functional groups at the edge of GO than in the plane. This has been validated by high-resolution transmission electron microscopy (HR-TEM), shown in Figure 2F. The HR-TEM image shows crystalline graphitic regions connected with an amorphous region, where the amorphous region represents the cross-linking (additional TEM, HR-TEM, and selected area electron diffraction data are provided in the Supporting Information). The same process for FGO results in similar macroscopic structure with a slightly different morphology, as shown in Figure 2E (additional FE SEM image is provided in the Supporting Information). As we proposed in our previous reports,[17,28] FGO has more oxygen functionalities at the edges and C−F bonds in the plane. This can result in cross-linking *via* the edges than plane, giving rise to large interconnected sheets with a smaller number of interplanar cross-linking. Hence, slight difference in the structures of poly-GO and poly-FGO may be due to the subtle difference in the surface chemistry of both GO samples. Poly-GO and poly-FGO retain all the functional groups of pristine GO powder as shown in the FTIR spectra (Figure 3A),[2,28,29] additionally showing an FTIR peak at 2900 cm^{-1} corresponding to the −CH stretching mode of the hemiacetal group. This provides another confirmation for cross-linking *via* GAD. All additional particulars of functional groups are reported in our previous work.[28,29]

Thermogravimetric analysis (TGA) of poly-GO in air atmosphere (Figure S4, Supporting Information) resembles that of GO. Moreover, only a small mass fraction has been disintegrated between 200 and 400 °C, indicating that the amount of the amorphous Res and GAD gel (which disintegrates mainly in this temperature window) is very small compared to GO.[30] The BET isotherm (Figure S5A,B, Supporting Information) appears to be categorized as a type IV isotherm associated with capillary condensation in mesopores before filling its majority macropore volume at higher relative pressures indicated by the steep slope as $P/P_0 = 1$. The hysteresis loop seems to be type B associated with slit-shaped pores, which makes sense due to the flake-like structure of GO. Low- and high-resolution TEM images showing the porosity in the interconnected GO sheets are shown in Supporting Information, Figure S6. Poly-GO has an average surface area of ∼700 m^2/g, and it has a broad range of meso- and macroporous distribution, identified from the cumulative pore distribution histogram (Figure S5C, Supporting Information). The bulk density of a perfectly shaped poly-GO sponge is evaluated as 0.02 g/cm^3 (∼100 times less than that of graphite). However, the skeletal density of poly-GO measured by helium pycnometry is found to be ∼0.8 g/cm^3. This large discrepancy in the density values is attributed to the large number of available macroscopic voids in the sample. Poly-FGO has a slightly smaller surface area of ∼470 m^2/g, with a similar BET isotherm like poly-GO (Figure S5D, Supporting Information).

The contact angle studies on a flat surface of poly-GO show superhydrophilic nature, immediately wetting the samples right after dropping the water on the specimen surface (Figure 3B). The porous section on the surface is shown on the right. The poly-GO sample is subjected to controlled reduction at 50 °C in hydrazine monohydrate atmosphere in a vacuum oven for 12 h. The SEM image of poly-RGO (Figure 4A) clearly shows that the resultant microstructure retains the 3D connectivity. Contact angle remains above 100° even
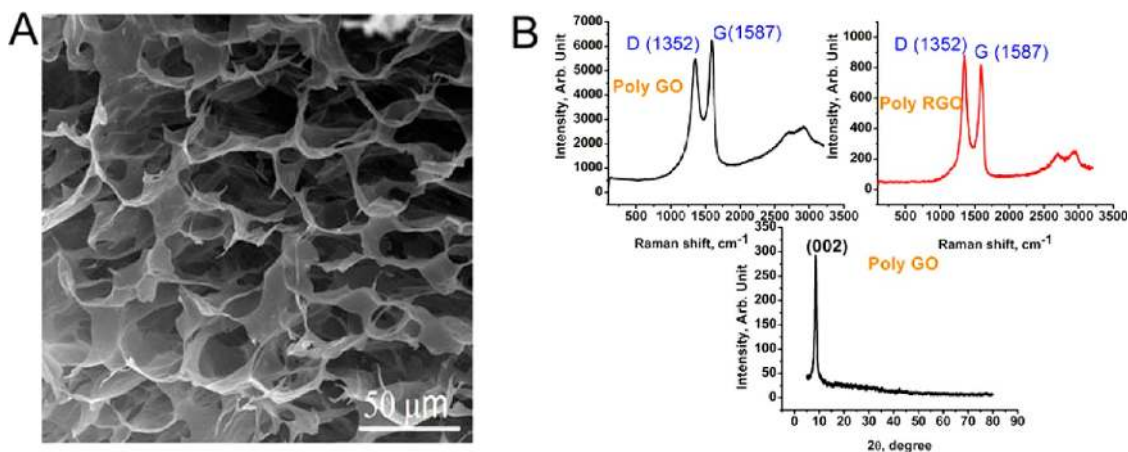
Figure 4. (a) SEM image of poly-RGO, subjected to controlled reduction at 50 °C in hydrazine monohydrate atmosphere in a vacuum oven. (b) Raman and XRD spectra of poly-GO and Raman spectra of poly-RGO.

after 5 min of water dropping, indicating the hydrophobic nature of the poly-RGO. Hydrophobic nature from these porous structures shows that the reduction has happened not just on the surface but also in the interior. Moreover, the FTIR of poly-RGO, as shown in the Figure 3A, reveals the reduction of functional groups. The other features of poly-GO, such as vibrational and structural characteristics analyzed by Raman spectra and powder XRD, respectively (Figure 4B), are found to be similar to that of GO. The decrease in the ratio of the intensities of G and D (I_G/I_D) in the Raman spectrum of poly-RGO is an indication of the reduction of GO, as noted by many other researchers in previous reports.[35] Further, from the XRD pattern of poly-GOs, the prominent (002) peak at ~10° indicates that the interplanar distance is still more than 6 Å, like pristine GO powders, even after the chemical treatments.

The bulk electrical conductivities of RGO powder and poly-RGO (tightly packed pellets) were evaluated using the four-probe method, which revealed conductivities of 1.63×10^{-3} and 3.4 S/m, respectively (Figures S8 and S9, Supporting Information). The reduction was carried out in a controlled fashion in the presence of hydrazine monohydrate reducing atmosphere created in a vacuum oven kept at 50 °C under a rotary vacuum for 12 h. This process enables the reduction of poly-GO successfully into poly-RGO as mentioned in Figures 3 and 4. Both GO powder and poly-GO were reduced under the same conditions. The conductivity value and the nature of the $I-V$ curve of RGO powder show that complete reduction has not happened in this case. However, in the case of poly-RGO, the $I-V$ curve shows conductive behavior (Figure S7B) and the conductivity value is 3 orders higher than that of RGO powder. Moreover, this conductivity lies in the range of reported conductivity values of RGO.[31] The porous nature of poly-GO has helped for the successful penetration of hydrazine vapor into the material and will help to enhance the extent of reduction. Moreover, the connectivity of individual RGO flakes in poly-RGO will

also contribute to the enhanced conductivity of poly-RGO.

CO2 Adsorption Measurements. CO_2 adsorption and desorption isotherms were obtained at three different temperatures (0, 25, and 50 °C) up to 20 atm pressure (Figure 5A,B). The sample has been activated by heating at 60 °C under high vacuum for 2 h. For the gas adsorption measurements on low density materials, it is extremely important to maintain the experimental conditions and use correct density values in order to obtain accurate uptake capacity. Extreme care has been taken in our measurements, by choosing the correct skeletal density (0.8 g/cm^3) of poly-GO, measured by helium pycnometry, to determine the amount of CO_2 adsorbed on the sample under isothermal conditions. Various precautions were taken to maintain the sample temperature constant during the entire process of adsorption and desorption cycles. Kinetics measurements were also performed on the sample at 22 atm pressure (Figure S10, Supporting Information). The freeze-dried poly-GO sample showed good uptake of CO_2 with high adsorption capacities compared to many other carbon-based materials.[32] At room temperature, poly-GO showed improved adsorption capacities (2.7 mmol/g at a pressure of 20 atm). The isotherms exhibit almost saturation behavior, similar to most of the carbon-based physisorption materials. The micro- and mesopores present in the 3D network seem to act efficiently as active sites for CO_2 adsorption. The obtained results show that several of the macropores do not really contribute to the adsorption capacities. In general, the higher the BET surface area, the higher the adsorption capacity. The isotherms follow a saturation behavior. Desorption measurements reveal good reversibility of CO_2 uptake. Desorption isotherms at different temperatures show similar behavior and are given in Supporting Information (Figure S10). The cross-linked 3D network of poly-GO results in maximizing the interaction potential between the CO_2 molecules and the GO surface.
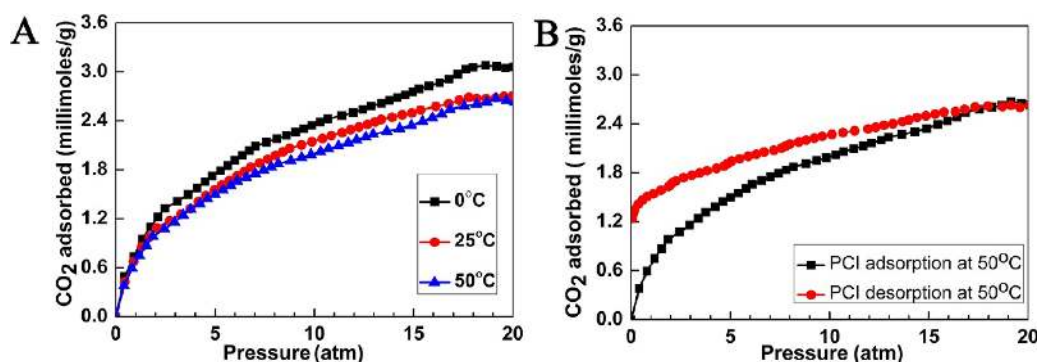
Figure 5. CO₂ adsorption measurements. (A) High pressure carbon dioxide excess adsorption isotherms collected at three different temperatures. (B) CO₂ adsorption and desorption isotherms at 50 °C.

Based on these observations, the mechanism of CO_2 absorption in poly-GO scaffolds is explained as follows: major contribution to the observed CO_2 adsorption capacity comes from the porous morphology, through van der Waals type weak interaction between the poly-GO network and CO_2 gas molecules. Good reversibility observed in the desorption measurements also indicates the role of weak van der Waals force involved in the sorption mechanism. Most of the macropores present in the material do not really contribute to the observed adsorption capacity. Apart from this, there could be a slight contribution to the CO_2 uptake from the chemical interaction between CO_2 molecules and the carbonyl functional groups present in the poly-GO sample. There are early reports on the formation and stability of complexes formed by the reaction between CO_2 and carbonyl compounds.[33,34]

CONCLUSION

To conclude, we have demonstrated the design and fabrication of poly-GO and its functional variations (*e.g.*, poly-FGO and poly-RGO), a completely cross-linked 3D network of GO, by polymerization using glutaraldehyde and resorcinol. Such macroscopic structures are found to keep their structural integrity up to 100 °C and can be easily tailored for different morphologies. The poly-GO sample exhibited good adsorption capacity for CO_2 storage, which is comparable (in some cases even exceeding) to other carbon-based nanoporous materials reported. Moreover, there are several advantages for carbon-based physical adsorbents over reported nanoporous materials like metal–organic frameworks (MOFs) and zeolites. Carbon-based nanoporous materials enable high amenability to pore structure modification and surface functionalization, relative ease of regeneration (*e.g.*, often very high regeneration temperatures are required for zeolites—a widely reported CO_2 sorbent), *etc.*, which are some of the important properties for good adsorbents. In addition, the 3D networked poly-GO sample reported in the present work is quite stable after several adsorption and desorption cycles, which is clearly an important advantage over many of the MOFs. Environmental benignity and low cost are some other important factors which make our material superior to MOFs and zeolites. These aerosol-like completely cross-linked 3D networks of macroscopic structures obtained by integrating 2D graphene oxide sheets can perhaps find use in high-performance systems for energy, environmental, and catalysis applications to name a few.

METHODS

Synthesis of GO. Graphene oxide was synthesized *via* an improved method.[35] For this, a 9:1 mixture of concentrated H_2SO_4/H_3PO_4 (360:40 mL) was added to a mixture of graphite flakes (3.0 g, 1 wt equiv) and $KMnO_4$ (18.0 g, 6 wt equiv). The reactants were then heated to 50 °C and stirred for 12 h. The reaction was cooled to room temperature and poured onto ice with 30% H_2O_2 (3 mL). The material was then washed in succession with 200 mL of water, 200 mL of 30% HCl, and 200 mL of ethanol (2 times). The material remaining after this multiple-wash process was coagulated with 200 mL of ether, and the resulting suspension was filtered over a PTFE membrane with a 0.22 μm pore size. Fluorinated GO (FGO) has also been prepared using a similar method taking fluorinated graphite as the starting material.

Synthesis of Poly-GO. Dry GO was dispersed in deionized water (5 mg/mL) and treated with resorcinol (11 mM), borax (0.06 mM), and glutaraldehyde solution (22 mM). The resulting viscous fluid-like material and the solution were sonicated for 3 h. The material was then freeze-dried using a lyophilizer for 24 h, resulting in the formation of poly-GO sample (Figure S1C). Similarly, the poly-FGO was made by taking chemically treated FGO as the starting material.

CO₂ Adsorption Measurements. High pressure CO_2 adsorption–desorption isotherms were collected on a pressure composition isotherm (PCI) measurement system (Advanced Materials Corporation, USA) for pressures up to 20 atm over a temperature range of 0 to 50 °C. The instrument is designed on the basis of a conventional Sieverts apparatus (Supporting Information, Figure S11). Extreme care has been taken in recording the isotherms by employing a third-order virial expansion equation of the Ideal gas law in calculating the amount of gas adsorbed from its pressure, temperature, and the occupied volume. Accurate calibration of the instrument was made before the adsorption measurements. Prior to the adsorption measurements,

the well grinded sample (approximately 200 mg) was degassed at 60 °C under high vacuum (~10^{-6} bar) for 2 h. This removes the adsorbed gas molecules, impurities, *etc.* from the sample surface and makes the surface active for CO_2 adsorption. TGA was performed to get the suitable initial activation temperature. Desorption and kinetics studies were also performed on the sample at different temperatures.

Conflict of Interest: The authors declare no competing financial interest.

Supporting Information Available: Schematic of the synthesis procedure, photographs of variously shaped poly-GO sponges, their formation mechanism, additional SEM, TEM micrographs, details of BET surface area measurements, dc electrical conductivity measurement details and data, schematic of gas sorption measurement setup, and adsorption/desorption isotherms. This material is available free of charge *via* the Internet at http://pubs.acs.org.

REFERENCES AND NOTES

1. Li, D.; Kaner, R. B. Graphene-Based Materials. *Science* **2008**, *320*, 1170–1171.
2. Gao, W.; Alemany, L. B.; Ci, L. J.; Ajayan, P. M. New Insights into the Structure and Reduction of Graphite Oxide. *Nat. Chem.* **2009**, *1*, 403–408.
3. Chen, C. X.; Wei, W.; Lv, W.; Su, F. Y.; He, Y. B.; Li, B.; Kang, F.; Yang, Q. H. A Graphene-Based Nanostructure with Expanded Ion Transport Channels for High Rate Li-Ion Batteries. *Chem. Commun.* **2012**, *48*, 5904–5906.
4. Hashim, D. P.; Narayanan, T. N.; Romo-Herrera, J. M.; Cullen, D. A.; Hahm, M. G.; Lezzi, P.; Suttle, J. R.; Kelkhoff, D.; Muñoz-Sandoval, A.; Ganguli, S.; *et al.* Covalently Bonded Three-Dimensional Carbon Nanotube Solids *via* Boron Induced Nanojunctions. *Sci. Rep.* **2012**, *2:363*, 1–8.
5. Romo-Herrera, J. M.; Terrones, M.; Terrones, H.; Dag, S.; Meunier, V. Covalent 2D and 3D Networks from 1D Nanostructures: Designing New Materials. *Nano Lett.* **2007**, *7*, 570–576.
6. Dreyer, D. R.; Park, P.; Bielawski, C. W.; Ruoff, R. S. The Chemistry of Graphene Oxide. *Chem. Soc. Rev.* **2010**, *39*, 228–240.
7. Singh, E.; Chen, Z.; Houshmand, F.; Ren, W.; Peles, Y.; Cheng, H. M.; Koratkar, N. Superhydrophobic Graphene Foams. *Small* **2013**, *9*, 75–78.
8. Biener, J.; Dasgupta, S.; Shao, L.; Wang, D.; Worsley, M. A.; Wittstock, A.; Lee, J. R. I.; Biener, M. M.; Orme, C. A.; Kucheyev, S. O.; *et al.* Macroscopic 3D Nanographene with Dynamically Tunable Bulk Properties. *Adv. Mater.* **2012**, *24*, 5083–5087.
9. Niu, Z.; Chen, J.; Hang, H. H.; Ma, J.; Chen, X. A. Leavening Strategy To Prepare Reduced Graphene Oxide Foams. *Adv. Mater.* **2012**, *24*, 4144–4150.
10. Jung, S. M.; Jung, H. Y.; Dresselhaus, M. S.; Jung, Y. J.; Kong, J. A Facile Route for 3D Aerogels from Nanostructured 1D and 2D Materials. *Sci. Rep.* **2012**, *2:849*, 1–5.
11. Wu, Z. S.; Yang, S.; Sun, Y.; Parvez, K.; Feng, X.; Müllen, K. 3D Nitrogen-Doped Graphene Aerogel-Supported Fe_3O_4 Nanoparticles as Efficient Electrocatalysts for the Oxygen Reduction Reaction. *J. Am. Chem. Soc.* **2012**, *134*, 9082–9085.
12. Zhu, Y.; Li, L.; Zhang, C.; Casillas, G.; Sun, Z.; Yan, Z.; Ruan, G.; Peng, Z.; Raji, A. R.; Kittrell, C.; *et al.* A Seamless Three-Dimensional Carbon Nanotube Graphene Hybrid Material. *Nat. Commun.* **2012**, *3*, 1225.
13. Brodie, B. C. On the Atomic Weight of Graphite. *Philos. Trans. R. Soc. London* **1859**, *149*, 249–259.
14. Geim, A. K; Novoselov, K. S. The Rise of Graphene. *Nat. Mater.* **2007**, *6*, 183–191.
15. Geim, A. K. Graphene: Status and Prospects. *Science* **2009**, *324*, 1530–1534.
16. Narayanan, T. N.; Gupta, B. K.; Vithayathil, S. A.; Aburto, R. R.; Mani, S. A.; Tijerina, J. T.; Xie, B.; Kaipparettu, B. A.; Torti, S. V.; Ajayan, P. M. Hybrid 2D Nanomaterials as Dual-Mode Contrast Agents in Cellular Imaging. *Adv. Mater.* **2012**, *24*, 2992–2998.
17. Chantharasupawong, P.; Philip, R.; Narayanan, T. N.; Sudeep, P. M.; Mathkar, A.; Ajayan, P. M.; Thomas, J. Optical Power Limiting in Fluorinated Graphene Oxide: An Insight into the Nonlinear Optical Properties. *J. Phys. Chem. C* **2012**, *116*, 25955–25961.
18. Lee, W. C.; Haley, C.; Lim, Y. X.; Shi, H.; Tang, A. L.; Wang, Y.; Lim, C. T.; Loh, K. P. Origin of Enhanced Stem Cell Growth and Differentiation on Graphene and Graphene Oxide. *ACS Nano* **2011**, *5*, 7334–7341.
19. Fujita, T.; Guan, P.; McKenna, K.; Lang, X.; Hirata, A.; Zhang, L.; Tokunaga, T.; Arai, S.; Yamamoto, Y.; Tanaka, N.; *et al.* Atomic Origins of the High Catalytic Activity of Nanoporous Gold. *Nat. Mater.* **2012**, *11*, 775–780.
20. Cong, H. P.; Ren, X. C.; Wang, P.; Yu, S. H. Macroscopic Multifunctional Graphene-Based Hydrogels and Aerogels by a Metal Ion Induced Self-Assembly Process. *ACS Nano* **2012**, *6*, 2693–2703.
21. Zhang, J.; Xie, Z.; Hill, A. J.; She, F. H.; Thornton, A. W.; Hoang, M.; Kong, L. X. Structure Retention in Cross-Linked Poly(ethylene glycol) Diacrylate Hydrogel Templated from a Hexagonal Lyotropic Liquid Crystal by Controlling the Surface Tension. *Soft Matter* **2012**, *8*, 2087.
22. Chen, W.; Li, S.; Chen, C.; Yan, L. Self-Assembly and Embedding of Nanoparticles by *In Situ* Reduced Graphene for Preparation of a 3D Graphene/Nanoparticle Aerogel. *Adv. Mater.* **2011**, *23*, 5679–5683.
23. Kim, S.; Zhou, S.; Hu, Y.; Acik, M.; Chabal, Y. J.; Berger, C.; Heer, W.; Bongiorno, A.; Riedo, E. Room-Temperature Metastability of Multilayer Graphene Oxide Films. *Nat. Mater.* **2012**, *11*, 544–549.
24. Zhang, J.; Cao, Y.; Feng, J.; Wu, P. Graphene-Oxide-Sheet-Induced Gelation of Cellulose and Promoted Mechanical Properties of Composite Aerogels. *J. Phys. Chem. C* **2012**, *116*, 8063–8068.
25. Worsley, M. A.; Pauzauskie, P. J.; Olson, T. Y.; Biener, J.; Satcher, J. H.; Baumann, T. F. Synthesis of Graphene Aerogel with High Electrical Conductivity. *J. Am. Chem. Soc.* **2010**, *132*, 14067–14069.
26. Park, S.; Dikin, D. A.; Nguyen, S. A.; Ruoff, R. S. Graphene Oxide Sheets Chemically Cross-Linked by Polyallylamine. *J. Phys. Chem. C* **2009**, *113*, 15801–15804.
27. Xu, Y.; Wu, Q.; Sun, Y.; Bai, H.; Shi, G. Three-Dimensional Self-Assembly of Graphene Oxide and DNA into Multifunctional Hydrogels. *ACS Nano* **2010**, *4*, 7358–7362.
28. Mathkar, A.; Narayanan, T. N.; Alemany, L. B.; Cox, P.; Nguyen, P.; Gao, G.; Chang, P.; Romero-Aburto, R.; Mani, S. A.; Ajayan, P. M. Synthesis of Fluorinated Graphene Oxide and Its Amphiphobic Properties. *Part. Part. Syst. Charact.* **2013**, *30*, 266–272.
29. Mathkar, A.; Tozier, D.; Cox, P.; Ong, P.; Galande, C.; Balakrishnan, K.; Reddy, A. L. M.; Ajayan, P. M. Controlled, Stepwise Reduction and Band Gap Manipulation of Graphene Oxide. *J. Phys. Chem. Lett.* **2012**, *3*, 986–991.
30. Hu, N.; Meng, L.; Gao, R.; Wang, Y.; Chai, J.; Yang, Z.; Kong, E. S.; Zhang, Y. A Facile Route for the Large Scale Fabrication of Graphene Oxide Papers and Their Mechanical Enhancement by Cross-Linking with Glutaraldehyde. *Nano-Micro Lett.* **2011**, *3*, 215–222.
31. Narayanan, T. N.; Liu, Z.; Lakshmy, P. R.; Gao, W.; Nagaoka, Y.; Sakthi Kumar, D.; Lou, J.; Vajtai, R.; Ajayan, P. M. Synthesis of Reduced Graphene Oxide-Fe_3O_4 Multifunctional Freestanding Membranes and Their Temperature Dependent Electronic Transport Properties. *Carbon* **2012**, *50*, 1338–1345.
32. Samanta, A.; Zhao, A.; Shimizu, G. K. H.; Sarkar, P.; Gupta, R. Post-Combustion CO_2 Capture Using Solid Sorbents: A Review. *Ind. Eng. Chem. Res.* **2012**, *51*, 1438–1463.

33. Nelson, M. R.; Borkman, R. F. *Ab Initio* Calculations on CO$_2$ Binding to Carbonyl Groups. *J. Phys. Chem. A* **1998**, *102*, 7860–7863.
34. Kazarian, S. G.; Vincent, M. F.; Bright, F. V.; Liotta, C. L.; Eckert, C. A. Specific Intermolecular Interaction of Carbon Dioxide with Polymers. *J. Am. Chem. Soc.* **1996**, *118*, 1729–1736.
35. Marcano, D. C.; Kosynkin, D. V.; Berlin, J. M.; Sinitskii, A.; Sun, Z.; Slesarev, A.; Alemany, L. B.; Lu, W.; Tour, J. M. Improved Synthesis of Graphene Oxide. *ACS Nano* **2010**, *4*, 4806–4814.